Peptide Folding Dynamics: A Time-Resolved Study from the Nanosecond to the Microsecond Time Regime

Mariano Venanzi,*,† Emanuela Gatto,† Gianfranco Bocchinfuso,† Antonio Palleschi,† Lorenzo Stella,† Chiara Baldini,‡ Fernando Formaggio,‡ and Claudio Toniolo‡

Department of Chemical Sciences and Technologies, University of Rome Tor Vergata, Via della Ricerca Scientifica, 00133 Rome, Italy, and Department of Chemistry, University of Padova, Via Marzolo 1, 35131 Padova, Italy

Received: May 19, 2006; In Final Form: July 19, 2006

Time-resolved spectroscopies, spanning from the nanosecond to the microsecond time regime, coupled with molecular mechanics calculations, allowed us to assess the most populated conformations in solution of a series of analogues of trichogin GA IV, a natural undecapeptide showing significant antimicrobial activity. This peptide is characterized by a high content of the conformationally constrained α-aminoisobutyric acid and by a glycine−glycine motif in the central part of the sequence. Nanosecond time-resolved fluorescence experiments were performed to determine the conformational properties of the peptide analogues in solution, while transient absorption measurements allowed us to study the peptide dynamics on the microsecond time scale. Because the peptides examined were functionalized by a fluorescent probe at the N-terminus and a nitroxide quencher placed along the backbone at three different positions, the distance-dependent fluorophore−quencher interaction was exploited to obtain a deeper insight into their three-dimensional structural and dynamical properties. Further information on the conformational and dynamical features was obtained by photophysical experiments as a function of the viscosity and polarity of the medium. Taken together, the results revealed a transition from an elongated, helical conformation to a family of compact, folded structures mimicking a helix−turn−helix motif, which may represent a model of the early steps of the protein hydrophobic collapse.

Introduction

Lipopeptaibols are a unique group of naturally occurring oligopeptides exhibiting interesting antimicrobial activity.[1,2] They possess a lipophilic acyl chain at the N-terminus, a high content of α-aminoisobutyric acid (Aib), and a 1,2-amino alcohol at the C-terminus. Owing to the *gem*-dimethyl substitution on the C^{α} atom, Aib is well-known to favor the formation of the tightly folded 3_{10}-helix[3] and β-turn[4] structures.[5] Within the family of lipopeptaibols, trichogin GA IV, the primary structure of which is *n*-Oct-Aib-Gly-Leu-Aib-Gly-Gly-Leu-Aib-Gly-Ile-Lol, where *n*-Oct- is *n*-octanoyl and Lol is leucinol, is the prototypical molecule. X-ray diffraction data have shown that the first four residues at the N-terminus attain a right-handed 3_{10}-helix, while the C-terminal segment, next to the Gly^5-Gly^6 motif, populates a right-handed α-helix.[6] As a result, an amphiphilic structure is obtained, with the four Leu, Ile, and Lol hydrophobic residues located on one side of the helix and the four Gly residues residing on the opposite side. NMR studies have suggested that the $3_{10}/\alpha$-helical mixed conformation is basically maintained in solution, although the C-terminal region might be in equilibrium with unordered states.[7,8] The hypothesis that Gly^5-Gly^6 would form a hinge point between the N-terminal 3_{10}-helix and the C-terminal α-helix has been also advanced.[7] Less attention has been devoted to the dynamic features of trichogin, despite its peculiar amino acid composition, characterized by 27% conformationally restricted Aib residues and 36% conformationally mobile Gly residues.

SCHEME 1: Primary Structures of the Trichogin GA IV Analogues Investigated and the Molecular Structures of the Fmoc Group and the TOAC Residue

Fmoc-Aib^1-Gly-Leu-Aib^4-Gly-Gly-Leu-Aib^8-Gly-Ile-Leu-OMe (F0)

Fmoc-**TOAC**-Gly-Leu-Aib-Gly-Gly-Leu-Aib-Gly-Ile-Leu-OMe (F0T1)

Fmoc-Aib-Gly-Leu-**TOAC**-Gly-Gly-Leu-Aib-Gly-Ile-Leu-OMe (F0T4)

Fmoc-Aib-Gly-Leu-Aib-Gly-Gly-Leu-**TOAC**-Gly-Ile-Leu-OMe (F0T8)

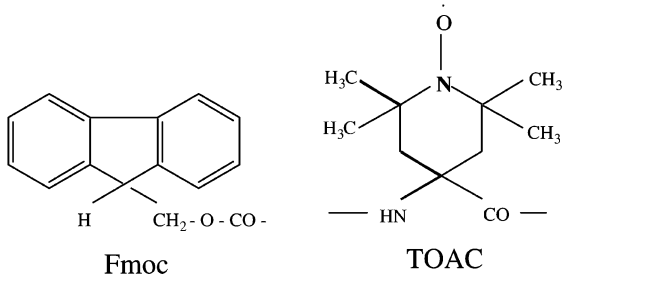

Fmoc TOAC

We synthesized a set of selected trichogin analogues with the aim at applying time-resolved spectroscopic techniques to investigate the three-dimensional structural and dynamical features of these peptides. The analogues examined, reported in Scheme 1, were functionalized by a fluorescent molecule (fluoren-9-ylmethyloxycarbonyl (Fmoc)) that replaces the *n*-octanoyl group of trichogin and by 4-amino-1-oxyl-2,2,6,6-tetramethylpiperidine-4-carboxylic acid (TOAC), a C^{α}-tetrasubstituted α-amino acid bearing a nitroxide radical species in its side chain. This latter residue was located along the backbone at different positions, replacing an Aib residue at position 1 in F0T1, at position 4 in F0T4, and at position 8 in F0T8. Thanks

* Author to whom correspondence should be addressed. Fax: (+39)-0672594328. E-mail: venanzi@uniroma2.it.
† University of Rome Tor Vergata.
‡ University of Padova

10.1021/jp063078w CCC: $33.50
Published on Web 10/25/2006

to these substitutions, F0T1 gauges the Fmoc···TOAC excited-state interaction at short distances, F0T4 the rigidity of the N-terminal segment preceding the Gly^5-Gly^6 central motif, and F0T8 the overall topology of the peptide chain. A further analogue, denoted F0 because it lacks the TOAC quencher, was also prepared as a reference compound for photophysical studies. Permeabilization experiments on phospholipid bilayers proved that these substitutions do not perturb the membrane activity of the lipopeptaibol (Supporting Information).

We have used time-resolved spectroscopy on the microsecond time scale for the study of the peptide chain dynamics, i.e., the interconversion kinetics among the most populated conformers. Different media, such as methanol (MeOH) and sodium dodecylsulfate (SDS) micelles, both secondary structure supporting, and the secondary structure disrupting 1,1,1,3,3,3-hexafluoropropan-2-ol (HFIP) have been also employed for this purpose, while the effect of viscosity on the kinetics of the conformational transitions has been investigated using a 8:2 (v/v) glycerol/methanol (Glc/MeOH) mixture.

Here, the photophysical and conformational properties of the three analogues F0T1, F0T4, and F0T8 are reported along with the dynamics through which F0T8 collapses from an elongated helix to a compact three-dimensional (3D) arrangement of the helix−turn−helix type. A preliminary account of the latter conformational transition has been already published.[9] However, a thorough investigation is now presented, focusing on the conformational pathways through which an elongated helix folds back, bringing two helical segments, separated by a flexible hinge point, into close proximity, thus mimicking the kinetics of relevant folding pathways occurring in globular proteins.

Experimental Section

The synthesis and chemical characterization of the Fmoc/TOAC trichogin GA IV analogues already have been reported.[10] UV and IR absorption experiments were performed on a Cary 100 spectrophotometer (Varian, Palo Alto, CA) and on a Nexus Fourier transform infrared (FTIR) spectrometer (Thermo-Nicolet, Madison, WI), respectively, the latter using CaF_2 cells. Circular dichroism (CD) experiments were carried out on a Jasco J-600 (Tokyo, Japan). Fluorescence spectra were recorded on a Fluoromax-2 (Jobin Yvon, Longjumeau, France) operating with single photon counting (SPC) detection ($\lambda_{exc} = 264$ nm). Quantum yields were obtained by using naphthalene in cyclohexane as a reference ($\phi_0 = 0.23 \pm 0.02$).[11] Fluorescence decays were measured using a CD900 SPC apparatus from Edinburgh Analytical Instruments (Edinburgh, U. K.). UV excitation ($\lambda_{exc} = 264$ nm) was achieved by a flashlamp filled with ultrapure hydrogen (300 mmHg; 40 kHz repetition rate; 1.1 ns full width at half-maximum). Experimental decay curves were fitted by a nonlinear least-squares analysis to multiexponential (ME) functions or lifetime distributions (TD) through an iterative reconvolution method by using standard software licensed by Edinburgh Instruments. All solutions for fluorescence experiments were freshly prepared and bubbled for 20 min with ultrapure nitrogen before measurement. Transient absorption experiments were performed with a LKS.60 (Applied Photophysics, Leatherhead, U. K.), using a Brilliant B Nd:YAG Q-switched laser (Quantel, Les Ulis, France) for pump excitation. A fourth harmonic generator module was employed to obtain a 266 nm excitation wavelength (4 ns pulse width; 10 mJ energy). Monochromatic probe light was obtained by filtering the output of a 150 W pulsed Xe lamp through two consecutive monochromators. Spectroscopic-grade solvents (Carlo Erba, Rodano, Italy) were used for all spectroscopic experiments. Molecular mechanics calculations were carried out by a homemade program interfaced with Hyperchem 7.0[12] using a MM+ force field implemented with the TOAC parameters.[13] Theoretical quenching efficiencies were calculated by positioning the fluorine transition dipole along the long axis of the aromatic plane,[14] while for the nitroxide group the absorption dipole was taken to be perpendicular to the NO bond and lying in the C−N−C plane, on the basis of the local C_s symmetry of the nitroxide group and the analogy to the $n \rightarrow \pi^*$ transition in carbonyls.[15]

Results and Discussion

Ground-State Properties: UV and FTIR Absorption and CD Measurements. The UV absorption spectral features of both Fmoc ($\lambda_{abs} = 264.5$ nm ($\epsilon = 2.0 \times 10^4$ M^{-1} cm^{-1}), 288.5 nm ($\epsilon = 5.0 \times 10^3$ M^{-1} cm^{-1}), 299.5 nm ($\epsilon = 5.9 \times 10^3$ M^{-1} cm^{-1})) and TOAC ($\lambda_{abs} = 240$ nm ($\epsilon = 2 \times 10^3$ M^{-1} cm^{-1}) and 460 nm (very weak, $\epsilon \approx 10$ M^{-1} cm^{-1})) in methanol are only slightly affected by the inclusion of the two chromophores in the peptide chain or by solvent effects, the absorption maxima of Fmoc in the analogues being shifted by 1−3 nm to longer wavelengths in Glc/MeOH and SDS and 1−2 nm to shorter wavelengths in HFIP. Furthermore, the sum of the absorption spectra of F0 and TOAC overlaps the spectra of F0T1, F0T4, and F0T8, ruling out the occurrence of strong ground-state interactions between the chromophores, even in the case of F0T1 despite their nearest neighbor positions.

FTIR absorption measurements of the peptides examined in $CDCl_3$ solution exhibit the well-known bands in the 3450−3300 cm^{-1} range, characteristic of amide N−H stretching vibrations, and in the 1750−1600 cm^{-1} range, associated with the stretching vibrations of carbonyl groups.[16,17] In particular, the spectra show an absorption band at 3330 cm^{-1}, typical of hydrogen-bonded N−H amide groups,[18] which predominates in all peptides investigated even at a concentration as low as 2×10^{-5} M (Supporting Information). The strong absorption of carbonyl groups in the region of 1662−1653 cm^{-1} at all concentrations examined, typical of hydrogen-bonded amide C=O groups, further supports the conclusion that intramolecularly hydrogen-bonded structures are largely populated in a structure-supporting solvent.

CD spectra in methanol, reported in Figure 1A, show a negative band at 204−206 nm and a weaker negative band at 222−229 nm, both being superimposable to those obtained by analogues of F0T1, F0T4, and F0T8 carrying an *n*-octanoyl group at the N-terminus.[19] These findings suggest that the substitution of the *n*-octanoyl moiety by Fmoc does not affect the conformational properties of the peptides and that the electronic transitions of the Fmoc group,[20] too remote from the nearest chiral center (the Leu^3 C^α atom), are not significantly optically active. Conversely, from the spectra reported in Figure 1A, it clearly appears that F0T4 and F0T8 adopt more constrained structures with respect to those of the natural trichogin GA IV[21] and both F0 and F0T1 analogues, suggesting a specific, structure-supporting role for the TOAC residue, depending on its position in the peptide chain.

CD studies have shown that many peptide helices unfold upon cooling when limited amounts of HFIP are added to the aqueous solution, because of preferential solvation of the peptide with the fluoro alcohol component ("solvent sorting").[22] Peptide unfolding induced by HFIP specific solvent effects is revealed by the CD spectra reported in Figure 1B. In particular, the CD spectrum of F0 is characteristic of a mostly unordered species, while the CD bands just above 200 nm of F0T1, F0T4, and

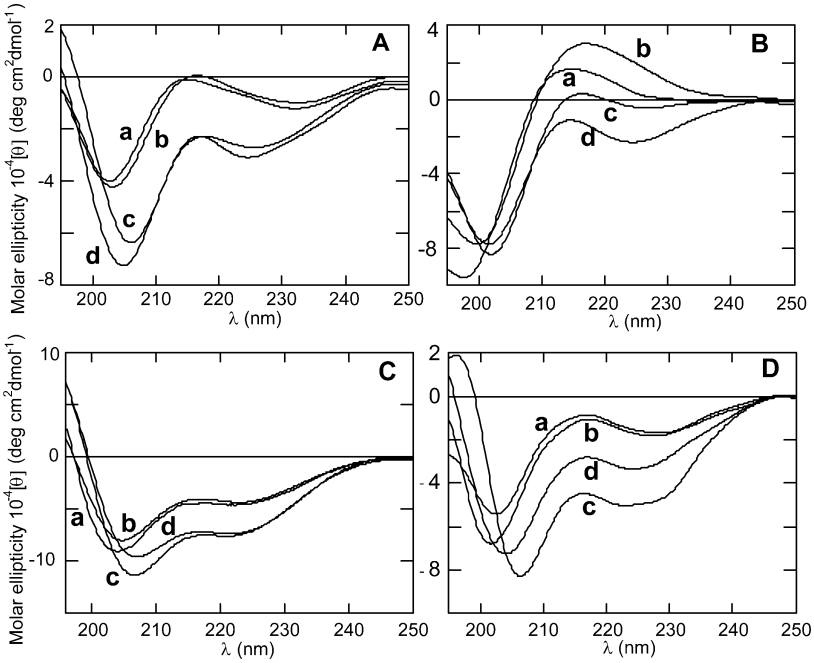

Figure 1. CD spectra of trichogin analogues (a) F0, (b) F0T1, (c) F0T4, and (d) F0T8 in (A) MeOH, (B) HFIP, (C) SDS, and (D) Glc/MeOH at $T = 25$ °C.

F0T8 suggest a somewhat more ordered structure. Moreover, according to the well-known structure-supporting properties of SDS micelles, the CD spectra of F0T4 and F0T8, reported in Figure 1C, show typical patterns of helical conformations.

Addition of glycerol to methanol is known to produce two main effects: (i) The interconversion dynamics among different conformers, as well as librational and large amplitude motions of the side chains, are markedly slowed, and (ii) ordered conformations are stabilized, probably because of solvent excluding effects. The latter effect is evident from the spectra in Figure 1D. In view of the higher viscosity of glycerol (945 cP at 298 K) as compared to that of methanol (0.55 cP at 298 K) and its sensitivity to the temperature, CD experiments in Glc/MeOH in the temperature range between 262 and 313 K were also carried out. These experiments show negligible temperature effects for all of the peptides investigated, implying that conformational equilibria in solution are not affected by solvent viscosity.

Excited-State Properties: Fluorescence and Transient Absorption Measurements. The fluorescence spectra reported in Figure 2 show that the Fmoc emission intensity in MeOH decreases along the series F0 > F0T8 > F0T4 > F0T1, thereby indicating the occurrence of a distance-dependent excited-state interaction between Fmoc and the nitroxide radical quencher. This finding was confirmed in all solvents employed, as inferred from the static quenching efficiencies reported in Table 1. This latter parameter was obtained by the fluorescence quantum yields of the Fmoc/TOAC peptides (ϕ) and of the reference compound F0 (ϕ_0), i.e., $E_{st} = [1 - (\phi/\phi_0)]$. Time-resolved fluorescence measurements in MeOH, HFIP, Glc/MeOH, and SDS solutions were also carried out (Table 2), the experimental time decays being described by a multiexponential function (ME), i.e.,

$$I(t) = \sum_{i=1}^{n} \alpha_i \exp\left(-\frac{t}{\tau_i}\right) \qquad (1)$$

where α_i is the weight associated to the ith lifetime component τ_i. From time-resolved experiments the average dynamic

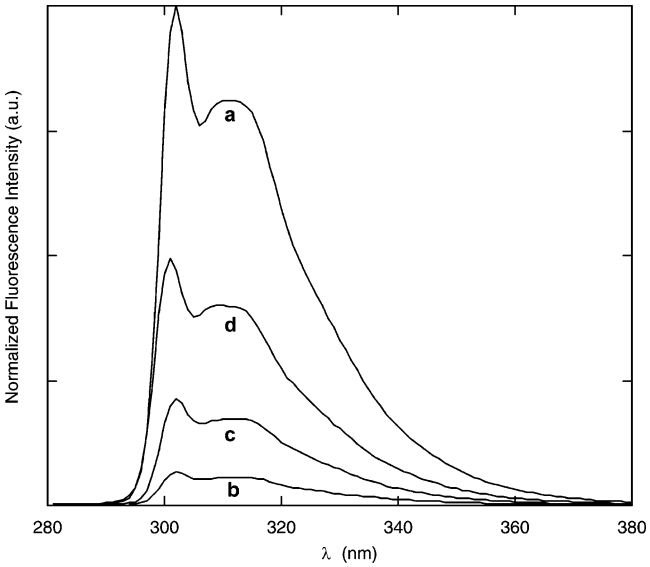

Figure 2. Fluorescence spectra in MeOH of trichogin analogues (a) F0, (b) F0T1, (c) F0T4, and (d) F0T8 at $T = 25$ °C.

quenching efficiency is given by $E_{dyn} = 1 - (\langle\tau\rangle/\tau_0)$, where

$$\langle\tau\rangle = \frac{\sum_i \alpha_i \tau_i}{\sum_i \alpha_i}$$

is the average decay time of the Fmoc/TOAC peptides and τ_0 is the F0 lifetime (Table 1). From the data reported in Table 1 it can be noted that the static quenching efficiencies are systematically higher than the dynamic ones for all peptides in all solvents investigated, the most notable difference being found for F0T8. In principle, this finding could be ascribed to the formation of a nonfluorescent ground-state complex or to an almost instantaneous excited-state interaction, the latter mechanism requiring the donor−acceptor pair at contact distances.

TABLE 1: Quantum Yield (ϕ), Average Lifetime ($\langle\tau\rangle$), Static (E_{st}) and Dynamic (E_{dyn}) Quenching Efficiencies for Trichogin GA IV Analogues in Different Solvents

solvent	peptide	ϕ	$\langle\tau\rangle$ (ns)	E_{st}	E_{dyn}
MeOH	F0	0.41 ± 0.03	9.0 ± 0.5		
	F0T1	0.03 ± 0.01	1.5 ± 0.1	0.93 ± 0.03	0.83 ± 0.02
	F0T4	0.09 ± 0.01	2.6 ± 0.1	0.78 ± 0.03	0.72 ± 0.02
	F0T8	0.20 ± 0.01	5.1 ± 0.4	0.51 ± 0.02	0.43 ± 0.01
HFIP	F0	0.40 ± 0.03	7.6 ± 0.4		
	F0T1	0.02 ± 0.01	0.8 ± 0.1	0.96 ± 0.03	0.89 ± 0.03
	F0T4	0.05 ± 0.01	1.4 ± 0.1	0.88 ± 0.03	0.82 ± 0.03
	F0T8	0.27 ± 0.02	6.3 ± 0.4	0.31 ± 0.02	0.17 ± 0.02
Glc/MeOH	F0	0.38 ± 0.03	7.6 ± 0.4		
	F0T1	0.06 ± 0.01	2.1 ± 0.1	0.84 ± 0.03	0.72 ± 0.03
	F0T4	0.13 ± 0.01	3.8 ± 0.2	0.67 ± 0.03	0.50 ± 0.02
	F0T8	0.26 ± 0.02	5.9 ± 0.6	0.31 ± 0.02	0.24 ± 0.02
SDS	F0	0.41 ± 0.03	8.6 ± 0.4		
	F0T1	0.03 ± 0.01	1.1 ± 0.1	0.93 ± 0.03	0.87 ± 0.03
	F0T4	0.07 ± 0.01	2.2 ± 0.1	0.83 ± 0.03	0.75 ± 0.03
	F0T8	0.20 ± 0.02	6.5 ± 0.6	0.52 ± 0.02	0.25 ± 0.02

TABLE 2: Fluorescence Time Decay Parameters (Lifetimes (τ_i) and Preexponents (α_i)) of Trichogin GA IV Analogues in Different Solvents as Recovered by Multiexponential (ME) and Lifetime Distribution (TD) Analyses[a]

solvent	sample	data analysis	α_1	τ_1 (ns)	α_2	τ_2 (ns)	α_3	τ_3 (ns)	χ^2
MeOH	F0T1	ME	0.86	0.5	0.14	7.9			1.02
		TD	0.84	0.5	0.16	7.9			1.00
				(±0.1)		(±0.6)			
	F0T4	ME	0.57	0.7	0.20	3.2	0.23	6.8	0.94
		TD	0.65	0.7	0.35	5.6			0.94
				(±0.4)		(±1.5)			
	F0T8	ME	0.15	1.6	0.60	4.8	0.25	7.8	1.09
		TD	0.15	1.7	0.85	5.7			1.10
				(±0.1)		(±1.4)			
HFIP	F0T1	ME	0.89	0.3	0.02	2.8	0.09	7.6	1.00
		TD	0.95	0.1			0.05	7.2	1.04
				(±0.1)				(±1.4)	
	F0T4	ME	0.80	1.0	0.14	2.1	0.06	5.6	1.18
		TD	0.93	1.1			0.07	5.8	1.22
				(±0.3)				(±1.2)	
	F0T8	ME	0.21	4.4	0.79	6.8			1.02
		TD			1	6.5			1.15
						(±1.1)			
Glc/MeOH	F0T1	ME	0.55	0.9	0.31	2.1	0.14	7.1	1.05
		TD	0.86	1.3			0.14	6.9	
				(±0.6)				(±0.9)	
	F0T4	ME	0.39	1.4	0.45	4.6	0.16	7.4	1.11
		TD	0.37	1.4	0.63	5.2			1.11
				(±0.2)		(±1.2)			
	F0T8	ME	0.20	2.6	0.80	6.7			1.10
		TD	0.16	2.3	0.84	6.6			1.10
				(±0.2)		(±0.7)			
SDS	F0T1	ME	0.70	0.4	0.24	1.3	0.06	8.5	1.01
		TD	0.93	0.7			0.07	8.3	
				(±0.4)				(±1.3)	
	F0T4	ME	0.60	1.3	0.32	2.6	0.08	7.2	1.14
		TD	0.80	1.6			0.10	6.6	
				(±0.7)				(±1.6)	
	F0T8	ME	0.20	3.6	0.80	7.2			1.17
		TD	0.11	3.4	0.89	6.9			
				(±0.2)		(±0.8)			

[a] Data in parentheses are distribution widths. τ_0(F0): 9.0 ns (MeOH); 7.6 ns (HFIP); 7.6 ns (Glc/MeOH); 8.6 ns (SDS).

Remembering that strong ground-state interactions were ruled out on the basis of the UV absorption results, it may be concluded that the two chromophores experience short-range interactions, very likely arising from a molecular rearrangement leading Fmoc and TOAC to close proximity.

From the data reported in Table 2, it easily can be seen that two or three lifetimes adequately describe the experimental time decays in all solvents used, despite the large difference in their physicochemical properties. F0T1 and F0T4 always show a predominantly short lifetime, while the F0T8 time decay is accounted for by a predominantly long decay time component. These results confirm the distance-dependent Fmoc/TOAC quenching mechanism and indicate that only a few conformers are actually populated in solution. Lifetime distribution analysis (TD) supports these conclusions, giving in all cases bimodal, narrow distributions. The sole exception is represented by F0T8 in HFIP, the time decay of which is described by a single lifetime distribution, denoting specific solvent effects, as also shown by CD experiments. It could be questioned which analysis (ME or TD) more correctly describes the experimental time decays. Let us discuss in detail the case of F0T8, the most sensitive to the peptide topological properties. In an organized medium such as SDS or in a highly viscous solvent such as Glc/MeOH ME and TD provided the same decay parameters, i.e., two lifetime components and two relatively narrow distributions characterized by very similar weights and time peak positions. In this case we can associate to each lifetime a specific conformer (ME) or a family of conformers exploring similar distances and orientations on the nanosecond time scale (TD). In MeOH the shorter lifetime distribution matches in weight and time peak position the shortest discrete lifetime. The width of this distribution is only a few percent of the peak value, so we can consider it sufficiently narrow to be equivalent to the shortest lifetime. The longer lifetime distribution takes into account the two longer time components, in that the weight of the distribution is the sum of the weights of the two lifetimes and its time peak occurs at the weighted average of the two lifetimes, i.e., $(0.60 \times 4.85 + 0.25 \times 7.84)/(0.60 + 0.25) = 5.73$. Extensive literature has been dedicated to the possibility of distinguishing between a large distribution and two discrete lifetimes solely on statistical grounds, i.e., analyzing the quality of the fitting parameters.[23]

An important insight to the problem comes from temperature-dependent time-resolved experiments in Glc/MeOH (Table 3). At all temperatures ME and TD analysis gave similar results, with only slight variations in the time decay parameters, altough the viscosity of the solution vary from 410 cP at 269 K to 50 cP at 313 K. In particular, the widths of the time distributions do not vary with the temperature and are always less than 10% of the peak value. In the case of a lifetime distribution coming from conformational heterogeneity, its width should have sensibly increased with increasing the solution viscosity.[24] These considerations also apply when comparing the decay parameters obtained for MeOH (η(298 K) = 0.55 cP) and Glc/MeOH (η-(298 K) = 100 cP. This important result strongly suggests that dynamic effects on the nanosecond time scale are definitely negligible and that ME analysis adequately describes the experimental time decays. This also means that it is possible to associate a specific conformer to each recovered lifetime.[25,26]

We next carried out transient absorption experiments, which provide information on the quenching process of the Fmoc triplet state by TOAC on the microsecond time scale.[27] Fmoc triplet state decays at 370 nm are reported in Figure 3 for all peptides examined, while the associated decay parameters, i.e., the normalized differential absorptions ($\Delta A/A$) and the triplet decay rate constants (k_T), are listed in Table 4. It is worth noting that the triplet state population, proportional to $\Delta A/A$ at $t = 0$, decreases parallel to the singlet state lifetime, because of the competition between the Fmoc/TOAC energy transfer process and

TABLE 3: Fluorescence Lifetimes (τ_i) and Preexponents (α_i) for Trichogin GA IV Analogues in Glc/MeOH at Different Temperatures from Multiexponential (ME) and Lifetime Distribution (TD) Analyses[a]

T (K)/[η (cP)]	sample	data analysis	α_1	τ_1 (ns)	α_2	τ_2 (ns)	α_3	τ_3 (ns)	χ^2
269/[410]	F0T1	ME	0.24	1.1	0.25	3.0	0.51	6.6	1.08
		TD	0.32	1.5 (±0.2)	0.68	5.9 (±1.2)			1.08
	F0T4	ME	0.26	1.4	0.27	3.9	0.47	7.0	1.10
		TD	0.29	1.6 (±0.3)	0.71	6.1 (±1.4)			1.11
	F0T8	ME	0.19	3.0	0.81	7.3			1.16
		TD	0.12	2.3 (±0.1)	0.88	7.1 (±0.9)			1.14
298/[100]	F0T1	ME	0.55	0.9	0.31	2.1	0.14	7.1	1.05
		TD	0.86	1.3 (±0.6)	0.14	6.9 (±0.9)			1.06
	F0T4	ME	0.39	1.4	0.45	4.6	0.16	7.4	1.11
		TD	0.37	1.4 (±0.2)	0.63	5.2 (±1.2)			1.11
	F0T8	ME	0.20	2.6	0.80	6.7			1.10
		TD	0.16	2.3 (±0.1)	0.84	6.6 (±0.7)			1.10
313/[50]	F0T1	ME	0.53	0.6	0.30	1.5	0.16	6.8	1.03
		TD	0.83	0.8 (±0.5)	0.17	6.6 (±1.1)			1.03
	F0T4	ME	0.36	1.3	0.32	3.7	0.32	6.5	1.09
		TD	0.39	1.3 (±0.5)	0.61	5.1 (±1.5)			1.10
	F0T8	ME	0.22	2.5	0.78	6.4			1.00
		TD	0.17	2.2 (±0.1)	0.83	6.3 (±0.7)			1.00

[a] Data in parentheses are distribution widths. τ_0(F0): 7.8 ns (269 K); 7.6 ns (293 K); 7.5 ns (313 K).

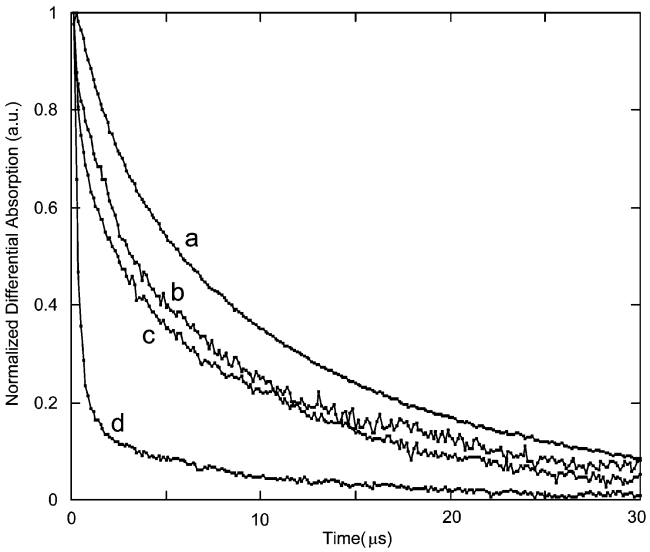

Figure 3. Transient absorption decays of trichogin analogues (a) F0, (b) F0T1, (c) F0T4, and (d) F0T8 ($\lambda = 370$ nm, MeOH, $T = 25$ °C).

the Fmoc singlet-to-triplet intersystem crossing. It also appears that F0T8 undergoes the fastest triplet decay, notably faster than those of F0T1 and F0T4, despite the longer Fmoc/TOAC separation in the primary structure. In addition, the F0T8 quenching rate constants in Glc/MeOH and SDS are markedly reduced, suggesting that the Fmoc triplet state relaxation is strongly affected by the peptide dynamics. Interestingly, the Fmoc triplet state decay of F0T8 in HFIP is not affected by the presence of the nitroxide quencher, indicating that in this environment the Fmoc···TOAC excited-state interaction is rather ineffective, as also shown by time-resolved fluorescence experiments.

TABLE 4: Fmoc Triplet State Decay Parameters and Rate Constants in Different Solvents

Fmoc Triplet State Decay Parameters for Trichogin GA IV Analogues in MeOH Solution ($\lambda = 370$ nm)

peptide	$\Delta A/A$	$(\Delta A/A)_{F0Tn}/(\Delta A/A)_{F0}$	$\langle\tau\rangle/\tau_0$[a]	$k_T \times 10^{-5}$ s^{-1}
F0	0.24			3.9
F0T8	0.15	0.63	0.57	34.9
F0T4	0.06	0.25	0.28	10.7
F0T1	0.03	0.12	0.18	6.4

Triplet State Decay Rate Constants in Different Solvents ($k_T \times 10^{-5}$ s^{-1})

	MeOH	Glc/MeOH	SDS	HFIP
F0	3.9	4.6	5.0	5.2
F0T8	34.9	17.7	11.8	6.0

[a] From time-resolved fluorescence experiments.

TABLE 5: Center-to-Center Distances (R_m), Orientation Factors (k_m^2), Theoretical (P_m) and Experimental (α_m) Populations, and Theoretical (E_m^{th}) and Experimental (E_m^{expt}) Quenching Efficiencies of the Most Stable Conformers of the Trichogin GA IV Analogues Investigated

peptide	R_m (Å)	k^2	P_m	α_m	E_m^{th}	E_m^{expt}
F0T1	6.4	0.465	0.87	0.86	0.95	0.95
	8.3	0.012	0.10	0.14	0.10	0.12
F0T4	9.4	2.027	0.50	0.57	0.90	0.93
	10.0	0.743	0.22	0.20	0.70	0.65
	8.4	0.247	0.21	0.23	0.69	0.25
F0T8[a]	14.7	0.847	0.37	0.60	0.17	0.47
	15.6	0.932	0.44	0.15	0.21	0.82
	13.8	0.482	0.19	0.25	0.18	0.13
A[b]	10.6	0.449	0.44	0.60	0.50	0.47
B	9.7	2.065	0.22	0.15	0.88	0.82
C	15.0	0.730	0.21	0.25	0.16	0.13

[a] Starting from the Gly^5-Gly^6 crystallographic structure. [b] Starting from 6^5 different conformations (see text).

Conformational Analysis and Molecular Modeling

The conformational features of the peptides investigated were also studied by molecular mechanics (MM) calculations. The energy minimization started from the mixed $3_{10}/\alpha$-helix structure of trichogin GA IV, as obtained by X-ray diffraction data,[6] analyzing the different rotational isomers of the Fmoc fluorophore and the two twisted-boat puckering conformations of TOAC.[28] The Boltzmann-weighted population (P_m), the Fmoc/TOAC center-to-center distance (R_m), and their relative orientations ($k_m^2 = \cos^2 \vartheta_m$ ($3 \cos^2 \gamma_m + 1$)) for the low-energy conformers of each peptide are reported in Table 5. In the k_m^2 orientation factor, ϑ_m and γ_m measure the angular displacement between the dipole transition vectors of the two probes in the mth conformer.[29]

In a series of papers we have shown that time-resolved fluorescence experiments and theoretical conformational analysis can be jointly applied for the determination of the conformational properties in a solution of sterically constrained oligopeptides (foldamers), suitably functionalized with energy transfer donor−acceptor pairs.[29,30] The photophysical relaxation mechanisms of the Fmoc/TOAC fluorophore/quencher pair have been recently investigated by us,[30] showing that for interchromophoric center-to-center distances longer than 4−5 Å the Förster dipole−dipole interaction model[31] adequately describes the excited-state interaction between the aromatic molecule and the nitroxyl radical quencher. At distances shorter than 4 Å, extensive overlap of the two electronic distributions occurs, and a Dexter

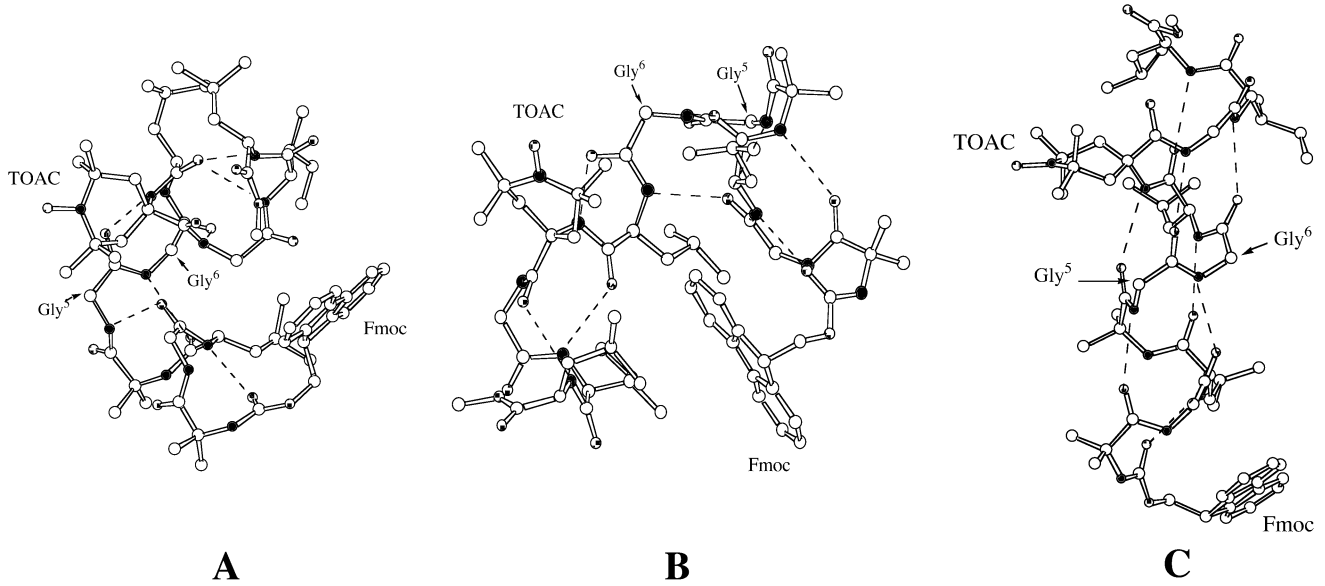

Figure 4. Ball-and-stick representation of the low-energy conformers (A−C) of F0T8. Carbon, empty circles; nitrogen, filled circles; oxygen, dotted circles. Hydrogen atoms are omitted for clarity. Dashed lines represent hydrogen bonds. Relative populations and geometric parameters for these structures are reported in Table 4.

energy transfer mechanism (electron exchange)[32] prevails, giving rise to an almost istantaneous quenching of the Fmoc excited state. Provided that the different conformers do not interconvert on the nanosecond time scale, so that dynamical averaging of the istantaneous relative positions of the donor and acceptor pair cannot take place, each decay time component can be associated to a specific conformer.[25] In this case the experimental quenching efficiency of the *m*th conformer is obtained from eq 2

$$E_m^{\text{expt}} = 1 - \frac{\tau_m}{\tau_0} \tag{2}$$

According to the Förster model, the energy transfer quenching efficiency is given by eq 3

$$E_m^{\text{th}} = \frac{1}{1 + \frac{2}{3k_m^2}\left(\frac{R_m}{R_0^*}\right)^6} \tag{3}$$

where R_m and k_m^2 are the aforementioned parameters and R_0^* represents the distance at which 50% transfer of excitation energy takes place.[33]

In the absence of ground-state interactions the experimental preexponential factor α_m can be directly related to the relative population P_m.[25] Therefore, a comparison of independently obtained experimental and theoretical results allows us to derive the basic structural features of the compounds examined in solution.

The data reported in Table 5 show a very satisfactory agreement between experimental and calculated quantities for F0T1 and F0T4, thus indicating that the N-terminal segment of the trichogin analogues preserves in solution the ordered arrangement of the crystal state and that the Fmoc and TOAC groups are constrained to a few, fixed relative orientations on the nanosecond time scale. In contrast, the calculated efficiencies of F0T8 are definitely lower than the experimental ones. For instance, the short lifetime varies between 1.6 ns (MeOH) and 4.4 ns (HFIP) (Table 2), giving rise to experimental quenching efficiencies varying between 0.42 and 0.82. Because the R_0^* parameter of the Fmoc/TOAC pair varies between 10.0 Å (Glc/MeOH) and 11.1 Å (HFIP), no elongated, helical structure can reproduce such high quenching efficiencies. Blocking the peptide backbone in a rigid, elongated helical conformation and exploring by MM calculations all of the possible conformations, we found that the minimum interprobe center-to-center distance is 13.4 Å. If we use this value in eq 3 and consider the appropriate value of R_0^* (10.9 Å in MeOH) and the highest experimental quenching efficiency ($E = 0.82$), then we obtain $k_m^2 = 10.5$, which is untenable (from its geometrical definition k_m^2 can vary between 0 and 4). These results strongly suggest that folded structures, characterized by relatively short through-space Fmoc/TOAC distances, in which the flexible, central Gly[5]-Gly[6] motif should play a pivotal role, significantly populate the solution.

A detailed molecular mechanics analysis of F0T8 was then performed. Energy minimization was carried out assuming 6^5 different starting structures generated by selecting 6 equally spaced values between 0 and 2π for the ϕ and ψ torsional angles of Gly[5] and Gly[6], the three most stable rotational isomers of Fmoc, and the two twisted-boat puckering structures of TOAC. Relative populations and geometrical parameters of the obtained most stable conformers (A, B, and C) of F0T8 are also reported in Table 5. The A and B conformations are both characterized by a compact 3D structure, in which the two N-terminal (1−4) and C-terminal (7−11) helical segments are brought to a close arrangement by the turn formed by the Gly[5]-Gly[6] residues, while the C conformer adopts an elongated, helical structure similar to that provided by X-ray diffraction data (Figure 4). A very satisfactory agreement between theoretical (P_m, E_m^{th}) and experimental (α_m, E_m^{expt}) parameters associated to the three conformers can be observed in Table 5. This finding validates the computed structures, all characterized by a high content of intramolecularly hydrogen-bonded residues. As already mentioned above, temperature-dependent time-resolved fluorescence experiments in Glc/MeOH showed that these conformers do not interconvert on the nanosecond time scale.

It should be stressed that the A, B, and C conformers account for the 87% of the overall theoretical population of the F0T8 conformers. High-energy computed structures, exhibiting center-to-center interchromophoric distances shorter than 4 Å, were

also found. These highly compact, minor structures are very likely responsible for the observed discrepancies between the static and the dynamic fluorescence quenching efficiencies previously reported.

If the picture provided by fluorescence time-resolved experiments is dynamically frozen, then peculiar dynamic effects are revealed by transient absorption measurements in the microsecond time region. First, the Fmoc triplet state decay in F0T8 is the fastest among all trichogin analogues and is strongly dependent on the viscosity (Glc/MeOH) and the environment (SDS micelles). However, the F0T1 triplet decay rate constant is the slowest despite the fact that Fmoc and TOAC are close in the primary structure. It is worth noting that in the F0T1 lowest-energy conformer Fmoc and TOAC are located on different sides of the 3_{10}-helix at a 6.4 Å center-to-center distance. One may therefore conclude that the through-bond Fmoc triplet state quenching by TOAC is rather inefficient for distances longer than a few angströms. Notably, the bimolecular quenching rate constant measured for the Fmoc/TOAC free molecules in solution almost reaches the diffusion limit ($k_q = 1.3 \times 10^9$ M^{-1} s^{-1}), implying that, as the Fmoc/TOAC pair approaches contact distances, the Fmoc triplet state is almost instantaneously quenched. We can conclude that quenching of the triplet state in the elongated, helical structure does not occur because of the relatively long Fmoc/TOAC distance, while in the bent 3D arrangement a short-range mechanism (electron exchange) gives rise to an almost instantaneous triplet state quenching every time the Fmoc/TOAC pair attains separation distances less than 4 Å.

It is worth having a closer look at the structural features governing the conformational equilibrium between the elongated helical conformation C and the compact conformers A and B. In the latter conformers the Aib[4]-Gly[5] sequence forms a β-bend type I, while the ϕ and ψ torsional angles of Gly[6] take values corresponding to a left-handed helical structure, thus driving the two terminal helical segments to collapse in a compact arrangement. The main differences between conformer C and the folded conformers A and B are observed for the ϕ and ψ torsional angles of Gly[6]. The energies of all conformers with energies less than 10 kcal mol^{-1} higher with respect to the lowest-energy conformation (A) are reported in Figure 5 as a function of the Gly[6] ϕ and ψ torsional angles. It can be noticed that the interconversion between the bent conformers A and B seems to require a relatively low activation energy, ϕ remaining at about the same value and ψ rotating by approximately 80°. The two-dimensional projection of the conformational energy map, also reported in Figure 5, reveals that high-energy conformations, some characterized by very short distances between Fmoc and TOAC, do occur in the same region of A and B. On the contrary, the transition from C to both A and B conformers ought to overcome a very high activation energy barrier, requiring a +120° large rotation about the ϕ torsional angle.

These findings lead us to adopt a very simple kinetic model able to explain both fluorescence (nanosecond regime) and transient absorption (microsecond regime) time-resolved experimental observations. We assume that (i) the C elongated, helical conformer slowly converts to the folded structures A and B on the microsecond time scale, (ii) the folded conformers A and B, which do not interconvert in the nanosecond time scale, show important dynamic effects in microseconds, passing through the family of compact conformers characterized by Fmoc/TOAC distances less than 4 Å, and (iii) a very fast (subnanosecond) singlet and triplet states quenching takes place

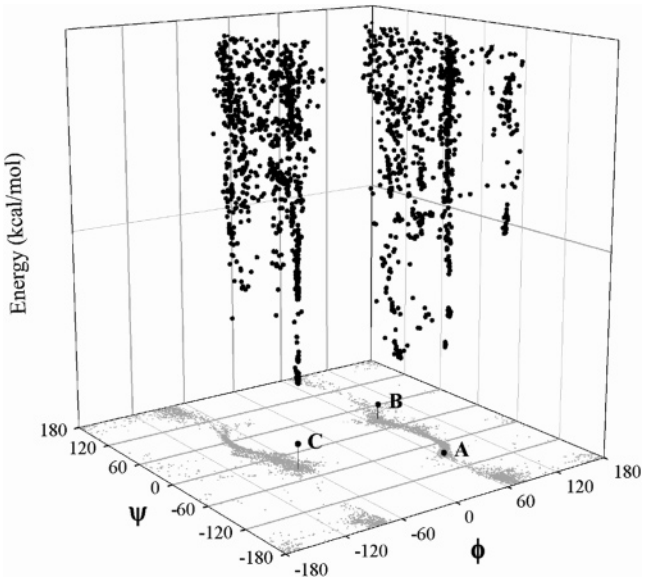

Figure 5. Conformational energies for the 6^5 different structures with energies less than 10 kcal mol^{-1} with respect to the lowest-energy conformer (A) as a function of the Gly[6] ϕ and ψ torsional angles. The projection in the (ϕ,ψ) plane shows the variety of high-energy conformations separating the A and B low-energy conformers.

with the highest efficiency in the compact conformations. This simple model explains both fluorescence results in the nanosecond regime (three not interconverting conformations, minor differences between static and dynamic quenching efficiencies, viscosity-independent fluorescence time decays) and microsecond transient absorption experiments (the dynamic effects observed for F0T8).

From the structural point of view the transitions leading from C to the other conformers involve the same activated torsional motion, i.e., a +120° rotation about the Gly[6] ϕ torsional angle. Actually, the observed triplet state quenching rate constant measures the rate of the torsional motion bringing the Fmoc/TOAC pair at close distances. From the data reported in Table 1, we obtain $k_{obs} = 3.12 \times 10^6$ s^{-1} (320 ns) for F0T8 in MeOH. This figure is intermediate between the diffusionally controlled rate of formation of end-to-end contacts in randomly coiled peptides (20−100 ns) and the 6−20 μs needed for the formation of a β-hairpin motif from peptide secondary structure units (α-helix or β-sheets).[34] In Glc/MeOH and SDS the triplet quenching efficiency notably decreases, the corresponding relaxation times (k_{obs}^{-1}) slowing down from 320 to 760 ns and 1.5 μs, respectively.

The F0T8 dynamics on the microsecond time scale are dominated by the interconversion from elongated, helical to compact, folded conformations, mimicking a helix−turn−helix arrangement. These considerations obviously do not apply to the photophysical relaxation of F0T1 and F0T4, which is not affected by this conformational transition primarily involving the relative motion of the two N- and C-terminal helical segments through the Gly[5]-Gly[6] hinge sequence.

Conclusions

The combined use of time-resolved spectroscopies and molecular mechanics calculations allowed us to characterize the conformational properties of a series of peptide analogues of trichogin GA IV in solution. While nanosecond time-resolved fluorescence experiments reveal the most populated conformers in solution, transient absorption measurements in the microsecond time regime account for the rate of the conformational

transition from elongated, helical to bent conformations, according to the distance-dependent excited-state interactions between the Fmoc fluorophore and the nitroxide-based quencher. Besides helical structures, such as those obtained by the X-ray diffraction analysis of trichogin GA IV, compact, folded conformations, generated by low-energy torsional motions about the Gly^5-Gly^6 central residues, are also populated in solution. These latter conformations do not occur in the solid state because of the energetically favored crystalline field arising from the close packing of the helical conformations. Interestingly, model peptides have been shown to successfully reproduce the folding kinetics of single-domain proteins.[35] The interconversion from elongated, helical conformations to the helix−turn−helix motif observed for F0T8 may actually mimic the early steps of the hydrophobic collapse switching on protein folding.

Acknowledgment. We thank Professor B. Pispisa (University of Tor Vergata) for many stimulating discussions. The financial contribution of MIUR (PRIN 2003) is also acknowledged.

Supporting Information Available: Peptide-induced leakage of carboxyfluorescein entrapped inside a liposome preparation and FTIR absorption of F0T8 in $CDCl_3$. This material is available free of charge via the Internet at http://pubs.acs.org.

References and Notes

(1) Rebuffat, S.; Goulard, Ch.; Bodo, B.; Roquebert, M. T. *Recent Res. Dev. Org. Bioorg. Chem.* **1999**, *3*, 65−91.

(2) Toniolo, C.; Crisma, M.; Formaggio, F.; Peggion, C.; Epand, R. F.; Epand, R. M. *Cell. Mol. Life Sci.* **2001**, *58*, 1179−1188.

(3) Toniolo, C.; Benedetti, E. *Trends Biochem. Sci.* **1991**, *16*, 350−353.

(4) Rose, G. D.; Gierasch, L. M.; Smith, J. P. *Adv. Protein Chem.* **1985**, *37*, 1−109.

(5) Toniolo, C.; Crisma, M.; Formaggio, F.; Peggion, C. *Biopolymers* **2001**, *60*, 396−419.

(6) Toniolo, C.; Peggion, C.; Crisma, M.; Formaggio, F.; Shui, X.; Eggleston, D. S. *Nat. Struct. Biol.* **1994**, *1*, 908−914.

(7) Auvin-Guette, C.; Rebuffat, S.; Prigent, Y.; Bodo, B. *J. Am. Chem. Soc.* **1992**, *114*, 2170−2174.

(8) Monaco, V.; Locardi, E.; Formaggio, F.; Crisma, M.; Mammi, S.; Peggion, E.; Toniolo, C.; Rebuffat, S.; Bodo, B. *J. Pept. Res.* **1998**, *52*, 261−272.

(9) Venanzi, M.; Gatto, E.; Bocchinfuso, G.; Palleschi, A.; Stella, L.; Formaggio, F.; Toniolo, C. *ChemBioChem* **2006**, *7*, 43−45.

(10) Monaco, V.; Formaggio, F.; Crisma, M.; Toniolo, C.; Hanson, P.; Millhauser, G. L. *Biopolymers* **1999**, *50*, 239−253.

(11) Eaton, D. F. *Pure Appl. Chem.* **1988**, *60*, 1107−1114.

(12) *Hyperchem Computational Chemistry*; Hyperchem, Inc.: Gainesville, FL, 2002.

(13) Barone, V.; Bencini, A.; Cossi, M.; Di Matteo, A.; Matterini, M.; Totti, F. *J. Am. Chem. Soc.* **1998**, *120*, 7069−7078.

(14) Michl, J.; Thulstrup, E. W. *Spectroscopy with Polarized Light*; VCH Publishers: New York, 1995; pp 402−406.

(15) Green, S. A.; Simpson, D. J.; Zhou, G.; Ho, P. S.; Blough, N. V. *J. Am. Chem. Soc.* **1990**, *112*, 7337−7346.

(16) Kennedy, D. F.; Crisma, M.; Toniolo, C.; Chapman, D. *Biochemistry* **1991**, *30*, 6541−6548.

(17) Pispisa, B.; Palleschi, A.; Stella, L.; Venanzi, M.; Mazzuca, C.; Toniolo, C.; Formaggio, F.; Broxterman, Q. B. *J. Phys. Chem. B* **2002**, *106*, 5733−5738.

(18) Mizushima, S.; Shimanouchi, T.; Tsuboi, M.; Souda, R. *J. Am. Chem. Soc.* **1952**, *74*, 270−271.

(19) Bui, T. T.; Formaggio, F.; Crisma, M.; Monaco, V.; Toniolo, C.; Hussain, R.; Siligardi, G. *J. Chem. Soc., Perkin Trans. 2* **2000**, 1043−1046.

(20) Yang, Z.; Gu, H.; Zhang, Y.; Wang, L.; Xu, B. *Chem. Commun.* **2004**, 208−209.

(21) Toniolo, C.; Crisma, M.; Formaggio, F.; Peggion, C.; Monaco, V.; Goulard, C.; Rebuffat, S.; Bodo, B. *J. Am. Chem. Soc.* **1996**, *118*, 4952−4958.

(22) Andersen, N. H.; Cort, J. R.; Liu, Z.; Sjoberg, S. J.; Tong, H. *J. Am. Chem. Soc.* **1996**, *118*, 10309−10310.

(23) Vix, A.; Lami, H. *Biophys. J.* **1995**, *68*, 1145−1151.

(24) Ferreira, S. T.; Stella, L.; Gratton, E. *Biophys. J.* **1994**, *66*, 1185−1196.

(25) Pispisa, B.; Palleschi, A.; Stella, L.; Venanzi, M.; Toniolo, C. *J. Phys. Chem. B* **1998**, *102*, 7890−7898.

(26) Pispisa, B.; Palleschi, A.; Mazzuca, C.; Stella, L.; Valeri, A.; Venanzi, M.; Formaggio, F.; Toniolo, C.; Broxterman, Q. B. *J. Fluoresc.* **2002**, *12*, 213−217.

(27) Lapidus, L. J.; Eaton, W. A.; Hofrichter, J. *Proc. Natl. Acad. Sci. U.S.A.* **2000**, *97*, 7220−7225.

(28) Crisma, M.; Deschamps, J. R.; George, C.; Flippen-Anderson, J. L.; Kaptein, B.; Broxterman, Q. B.; Moretto, A.; Oancea, S.; Jost, M.; Formaggio, F.; Toniolo, C. *J. Pept. Res.* **2005**, *65*, 564−579.

(29) Pispisa, B.; Palleschi, A.; Venanzi, M.; Zanotti, G. *J. Phys. Chem.* **1996**, *100*, 6835−6844.

(30) Pispisa, B.; Mazzuca, C.; Palleschi, A.; Stella, L.; Venanzi, M.; Wakselman, M.; Mazaylerat, J.-P.; Rainaldi, M.; Formaggio, F.; Toniolo, C. *Chem.—Eur. J.* **2003**, *9*, 4084−4093 and references therein.

(31) Förster, T. *Discuss. Faraday Soc.* **1959**, *27*, 7−17.

(32) Dexter, D. L. *J. Chem. Phys.* **1953**, *21*, 836−850.

(33) In eq 3 R_0^{*6} is defined as $2/(3k^2)R_0^6$, where R_0 is the Förster distance, as usually introduced in the fluorescence resonance energy transfer literature. We prefer our formulation of eq 3, because R_0^* depends only on spectral properties of the donor−acceptor pair and k^2 explicitly compares in the definition of the quenching efficiency.

(34) Eaton, W. A.; Muñoz, V.; Hagen, S. J.; Jas, G. S.; Lapidus, L. J.; Henry, E. R.; Hofrichter, J. *Annu. Rev. Biophys. Biomol. Struct.* **2000**, *29*, 327−359.

(35) Kubelka, J.; Hofrichter, J.; Eaton, W. A. *Curr. Biol.* **2004**, *14*, 76−88.